Computational Estimation of Lanthanoid−Water Bond Lengths by Semiempirical Methods

Michael Seitz* and Nicola Alzakhem

Department of Chemistry and Biochemistry, Ruhr-University Bochum, Universitätsstr. 150, D-44801 Bochum, Germany

Abstract: Over 650 lanthanoid complexes with Ln−OH$_2$ motifs have been modeled by the three semiempirical methods (AM1, PM3, or PM6)/SPARKLE. The geometrical deviations from the corresponding crystal structures can be described by normal distributions. Statistical inference analysis shows that AM1/SPARKLE is surprisingly accurate for the estimation of the average bond lengths Ln−OH$_2$ for the technologically important central lanthanoids (Ln = Eu−Tb) in complexes with pyridine-like ligands with a worst-case error of only 4.9%.

One of the most important structural elements in lanthanoid coordination chemistry is the Ln−OH$_2$ motif.[1] The nature and the geometrical arrangement of this ubiquitous feature has major implications for the use of lanthanoid complexes in a number of technologically important applications such as magnetic resonance imaging (MRI)[2−7] or lanthanoid luminescence.[8−14] The interactions between water molecules and Ln^{3+} cations are predominantly dipole−dipole in nature, for example, relaxation of proton nuclear spins in MRI or quenching of lanthanoid luminescence by O−H oscillators. Because of the strong distance dependence of these phenomena (proportional to r^{-6}) the geometric features of Ln−OH$_2$ bonds are critically important and various techniques have been used for their characterization. Most of them have been indirect methods, for example, using measured Ln−O distances from X-ray data or fitting NMRD profiles.[2−7] A few attempts, however, have also been made toward direct measurements, for example, with pulsed ENDOR studies.[15]

An alternative approach is the use of computational methods. Modeling lanthanoid complexes with sizes realistic for applications (often >100 atoms) is challenging. While ab initio methods are available, the high computational cost is often prohibitive. A more cost-effective alternative are semiempirical methods. In this context, the so-called "SPARKLE model" has allowed enormous progress in recent years for complexes with N- and O-donor ligands and has been implemented in a number of methods, including AM1,[16−18,20−29] PM3,[19−30] and PM6.[31,32] Regarding accuracy, their overall performance has been found to be comparable to ab initio calculations, while being hundreds of times faster and therefore allowing the modeling of rather large (>200 atoms) lanthanoid complexes.[33] In this paper, we report our preliminary findings on the semiempirical

modeling of two important classes of complexes with a special focus on the Ln−OH$_2$ fragments, a comparison regarding the performance of the different methods using statistical inference, and as the main result, the implications of the obtained findings for the computational estimation of lanthanoid−water bond lengths.[34]

In our investigation, we were not primarily interested in the ability of the different semiempirical methods to reproduce the overall geometric features (coordination polyhedron, all bond lengths, etc.) as closely as possible to the real situation,[34] which is usually the aim of computational method developers. Instead, the rather narrow goal was to find out whether semiempirical methods could be appropriate tools to accurately predict Ln−OH$_2$ bond lengths[35] in lanthanoid complexes, as well as to establish reasonable error estimates on the obtained values using statistical inference, which is potentially of great value for the coordination chemist.

The basic hypotheses for our investigation were as follows: (1) A specific semiempirical method has intrinsic inaccuracies that are characteristic and predetermined for a certain ligand type (e.g., H$_2$O, pyridines, etc.). (2) These inaccuracies manifest themselves in a specific (but unknown) statistical distribution around an average deviation relative to the crystal structures. (3) The unknown distributions can be estimated by sampling (i.e., modeling of a number of complexes and comparison to the respective known structures) and extrapolation using inferential statistics methodology. (4) From the obtained data, standard statistical methods can be used to determine certain parameters, like worst-case errors on calculated bond lengths.

The practical implementation within this framework started with the following basic idea: The sum S of all bond lengths around a trivalent lanthanoid center can be approximated with eq 1 which has been experimentally validated recently.[36]

$$S(r_{L,i}; m, x) \approx \left(\sum_{i=1}^{m} r_{L,i} \right) + mr_0 - \frac{mr_0(1-k)}{Z_0^*}x + \frac{mr_0(1-k)^2}{(Z_0^*)^2}x^2 \quad (1)$$

where $r_{L,i}$ is the radius of ligating atom i, m is the coordination number, x is the number of f-electrons, r_0 is the ionic radius (Slater) of La^{3+}, k is the screening constant for one f-electron, and Z_0^* is the effective nuclear charge of La^{3+}.

For a specific ligand system ($r_{L,i}$ and m constant) and a certain lanthanoid center (x = const.), the sum S should be constant, which is naturally the case when comparing calculated structures with crystal structures of the same complex. This, on the other hand, implies for a good computational model a negative correlation of the deviations in the bond lengths, that is, an elongation in one set of bond lengths must be compensated for by a shortening in the remaining other distances and vice versa. With the hypothesis that a semiempirical model has characteristic intrinsic inaccuracies for specific classes of ligands, it is obvious that the errors in the calculated Ln−OH$_2$ distances will depend

* To whom correspondence should be addressed. E-mail: michel-seitz@web.de.

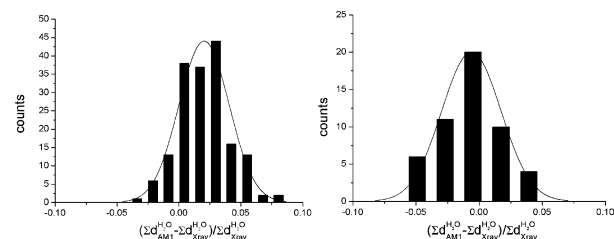**218** *J. Chem. Inf. Model.*, Vol. 50, No. 2, 2010

LETTER

Chart 1. Minimal Structural Criteria for the CSD Database Search: Pyridine-like (**1**, left) and Cyclen-Derived (**2**, right) Lanthanoid Complexes[a]
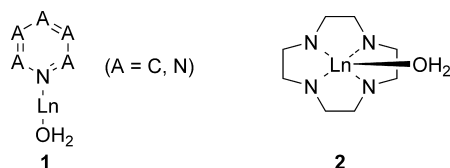
a Additional substitution was allowed at every position.

Table 1. Statistical Data for the Relative Deviations of the Calculated Average Bond Lengths Compared to the Crystal Structure Values

method, bond-type	N^a	$\bar{x} = \dfrac{\sum_i x_i}{N}$ [b]	$s = \sqrt{\dfrac{\sum_i (x_i - \bar{x})^2}{N-1}}$
		pyridine-like **1**	
AM1, Ln−OH$_2$	172	0.0204	0.0203
AM1, Ln−N$_{arom}$	172	−0.0167	0.0183
PM3, Ln−OH$_2$	172	0.0336	0.0185
PM3, Ln−N$_{arom}$	172	−0.0247	0.0159
PM6, Ln−OH$_2$	172	0.0321	0.0209
PM6, Ln−N$_{arom}$	172	−0.0313	0.0194
		cyclen-derived **2**	
AM1, Ln−OH$_2$	51	−0.0061	0.0235
AM1, Ln−N$_{cycl}$	51	−0.0263	0.0180
PM3, Ln−OH$_2$	51	0.0153	0.0205
PM3, Ln−N$_{cycl}$	51	−0.0335	0.0131
PM6, Ln−OH$_2$	51	0.0061	0.0201
PM6, Ln−N$_{cycl}$	51	−0.0436	0.0179

a N = number of structures in set. *b* $x = \{[(\Sigma d_{method}^{bond\text{-}type}) - (\Sigma d_{Xray}^{bond\text{-}type})]\}/\Sigma d_{Xray}^{bond\text{-}type}$.

Figure 1. Histograms for the relative deviations of the average Ln−OH$_2$ distances from the crystal structure values in complexes with pyridine-like ligands **1** (left) and cyclen-derived ligands **2** (right) as calculated by AM1.

strongly on the nature of the other ligands and their inherent inaccuracies. Therefore, our sampling strategy was to identify sets of lanthanoid complexes that are characterized, in addition to the Ln−OH$_2$ motifs, by the presence of mainly only one other class of similar ligating atoms to minimize the number of competing effects. Ultimately, we chose two important families of lanthanoid complexes with a great number of crystal structures deposited in the Cambridge Structural Database (CSD).[37] The first class is composed of complexes with pyridine-like ligands[38] (i.e., six-membered aromatic N-heterocycles like pyridines, pyrimidines, pyrazines, etc.); the second set features ligands with the cyclen motif[39] (e.g., derivatives of DOTA, DO3A, etc.), both being among the most used structural building blocks for lanthanoid coordination chemistry and its technologically important applications. Chart 1 shows the minimal structural requirements[40] that were used to retrieve the corresponding crystal structures from the CSD database as the starting points for the computational investigation.

The database searches yielded 172 structures for **1** and 51 for **2**. Both sets are reasonably large to allow for the statistical analysis of all lanthanoids combined and, in the case of **1**, even for individual lanthanoids (6 ≤ number of

structures ≤25). The crystal structures were used to create initial input geometries for the semiempirical calculations (AM1/SPARKLE, PM3/SPARKLE, PM6/SPARKLE),[41] which were performed using the MOPAC 2009[42] package.[43] The obtained sets of over 650 structures were analyzed with respect to the deviations in three different classes of bond lengths (Ln−OH$_2$ in **1** and **2**, Ln-N$_{arom}$ in **1** and N$_{cycl}$ in **2**) with respect to the relative average deviations (relative and absolute) compared to the crystal structure values. Table 1 shows the basic statistical data for the relative deviations of all lanthanoid complexes.[43]

As can be seen in Table 1, the mean deviations in Ln−OH$_2$ (except for **2**/AM1) are toward longer bond lengths compared to the crystal structure values, while the calculated values for both Ln−N distances tend to be too short.

Standard tests for normality (Shapiro−Wilk[44] or Lilliefors[45]) show that for the deviations in Ln−OH$_2$, the null hypothesis "data derived from a normally distributed population" cannot be rejected on a significance level of α = 0.05. For an additional visual inspection, histograms were constructed using Scott's efficient and unbiased bin size,[46] which also support the assumption of normally distributed deviations. Representative examples are shown in Figure 1.[42]

For a realistic estimation of the errors in the calculated deviations, the statistical spread of the sample means and the sample standard deviations have to be taken into account. With the assumption of normality of the underlying distributions, standard statistical inference procedures were employed to calculate confidence intervals for the sample means and sample standard deviations using the central *t*-distribution and the central χ^2-distribution, respectively, on a 99% confidence level for all lanthanoids combined (see Table 2) and on a 95% level for individual lanthanoids.[43]
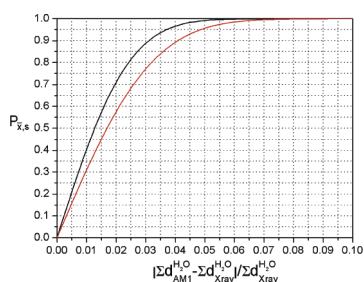
As can be seen in Table 2, for all lanthanoids combined, AM1 is the best method for complexes with pyridine-like ligands (**1**), whereas PM6 is outperforming the other two methods in cyclen-derived species (**2**). The results for the two classes cannot be directly compared due to the difference in sample sizes.[47] In addition, the worst-case errors for one individual lanthanoid can still be considerably larger than the average value listed in Table 1 because of the individual parametrization for each lanthanoid.

Therefore, rather than the overall accuracies, one would ideally like to know the maximal error for a specific lanthanoid on a certain confidence level. For this purpose, cumulative probability distributions as a function of the unsigned deviation from the crystal structure values were constructed for each lanthanoid individually with pyridine-like **1**[48] on the basis of a statistical worst-case scenario for the parameters sample mean and sample standard deviation

LETTER

J. Chem. Inf. Model., Vol. 50, No. 2, 2010 **219**

Table 2. Confidence Intervals (CI) for the Sample Means $\bar{x}$ and the Sample Standard Deviations s of the Relative Deviations of the Calculated Average Bond Lengths Ln−OH$_2$ Compared to the Crystal Structure Values, As Well As Estimates for the Worst-Case Errors

method	99% CI for $\bar{x}$ (central t-distr.)[a]		99% CI for s (central χ^2-distr.)[a]		worst-case error[b]
pyridine-like **1**					
AM1	0.0164	0.0244	0.0178	0.0235	0.064
PM3	0.0299	0.0373	0.0162	0.0215	0.073
PM6	0.0279	0.0363	0.0183	0.0242	0.077
cyclen-derived **2**					
AM1	−0.0149	0.0027	0.0186	0.0314	0.068
PM3	0.0076	0.0230	0.0163	0.0274	0.069
PM6	−0.0014	0.0136	0.0159	0.0269	0.054

[a] For the definitions of $\bar{x}$ and s, see Table 1. [b] Calculated using the sample mean furthest from zero and maximum standard deviation (see Supporting Information 1) on a significance level $\alpha = 0.05$, that is, 95% certainty that the real average value for Ln−OH$_2$ (from crystal structures) lies within the confidence interval [av $d_\text{method} \times$ (1-tabulated value); av $d_\text{method} \times$ (1 + tabulated value)].

Table 3. Statistical Worst-Case Errors for the Relative Deviations of the Calculated Average Bond Lengths Ln−OH$_2$ in **1**

f-el.	N^a	AM1 (%)[b]	PM3 (%)[b]	PM6 [%][b]
0	25	7.7	7.2	8.7
1	8	11.6	11.0	11.7
2	8	13.0	12.2	12.6
3	8	8.3	9.7	9.1
5	6	9.9	10.2	11.2
6	23	5.1	8.5	6.3
7	18	6.4	7.3	7.6
8	10	7.1	9.0	11.4
9	6	11.6	14.3	16.4
10	10	6.4	9.7	10.3
11	15	7.5	8.8	7.0
12	6	9.0	13.3	12.0
13	13	4.9	7.9	7.4
14	16	6.5	8.1	9.1
6−8	51	4.9	7.2	6.6

[a] N = number of structures in set. [b] Calculated using the sample mean furthest from zero and maximum standard deviation (see Supporting Information 1) on a significance level $\alpha = 0.05$, that is, 95% certainty that the real average value for Ln−OH$_2$ (from crystal structures) lies within the confidence interval [av $d_\text{method} \times$ (1 − tabulated value/100%); av $d_\text{method} \times$ (1 + tabulated value/100%)].

Figure 2. Cumulative probability density functions for the distributions of the relative deviations of the calculated (AM1) average Ln−OH$_2$ bond lengths (Ln = Eu, Gd, Tb) in **1** as found in the sample set (black) and in a statistical worst-case scenario (red) (see Table 3, last row).[43]

Figure 3. Worst-case errors for the calculated relative deviations (in %) of the average bond lengths Ln−OH$_2$ in **1** by lanthanoid (data points connected by splines solely for better clarity).

($\bar{x}$ with highest absolute value and maximal s). Figure 2 shows a representative example of a typical cumulative probability distribution function.[43] Table 3 summarizes the obtained errors for each lanthanoid.

A graphical representation of the errors listed in Table 3 succinctly illustrates the obtained results (Figure 3).
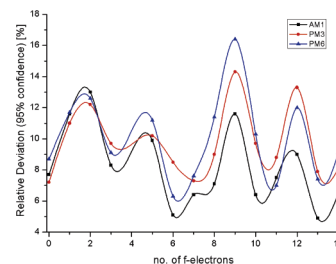
The results for complexes with pyridine-like ligands **1** are the following: In general, AM1 is an at least equal or better choice than PM3 or PM6. The errors for the light (La−Sm) and the heavy lanthanoids (Dy−Lu, except Tm/AM1 and Ho/AM1) are rather high and not very useful for the accurate estimation of Ln−OH$_2$ distances. The central lanthanoids (Eu, Gd, Tb) on the other hand, which are very important for a number of applications, have surprisingly small errors (5−7%). Statistics can even be improved by combining the three lanthanoid sets into one yielding a maximal error of only 4.9% (Table 3 last row and Figure 2).

In conclusion, we have shown the following: (1) The deviations of the calculated average bond lengths from the crystal structure values for three different classes of ligands are characteristic for a specific semiempirical method and can be assumed to be normally distributed. (2) Regarding the overall accuracies for Ln−OH$_2$ (Ln = La−Lu) distances, AM1/SPARKLE is the best method for complexes with pyridine-like ligands **1**, whereas PM6/

SPARKLE performs best for cyclen-derived species **2**. Both still show rather high error values and can not be recommended as generally applicable methods. (3) The worst-case errors in **1** for individual lanthanoids are generally quite high ($\geq$10%), especially for the light and heavy lanthanoids, which is not very useful for the computational estimation of Ln−OH$_2$ bond lengths. (4) AM1/SPARKLE performs well for the very important central lanthanoids Eu, Gd, and Tb, with worst-case errors of only 4.9%. This result makes AM1/SPARKLE a good tool for the computational estimation of Ln−OH$_2$ bond lengths (Ln = Eu, Gd, Tb) in complexes with pyridine-like ligands **1**, which is potentially very useful for the design and the rational development of functional lanthanoid complexes, for example, for Gd-based MRI contrast agents.[49]

Supporting Information Available: Tables of raw and processed data, details for the statistical evaluation, and full

graphical representations. This material is available free of charge via the Internet at http://pubs.acs.org.

REFERENCES AND NOTES

(1) Parker, D.; Dickins, R. S.; Puschmann, H.; Crossland, C.; Howard, J. A. K. Being Excited by Lanthanide Coordination Complexes: Aqua Species, Chirality, Excited-State Chemistry, and Exchange Dynamics. *Chem. Rev.* **2002**, *102*, 1977–2010.

(2) Toth, E.; Helm, L.; Merbach, A. E. Relaxivity of Gadolinium(III) Complexes: Theory and Mechanism. In *The Chemistry of Contrast Agents in Medical Magnetic Resonance Imaging*; Merbach, A. E., Toth, E., Eds.; Wiley: New York, 2001; pp 45−119.

(3) Caravan, P.; Ellison, J. J.; McMurry, T. J.; Lauffer, R. B. Gadolinium(III) Chelates as MRI Contrast Agents: Structure, Dynamics, and Applications. *Chem. Rev.* **1999**, *99*, 2293–2352.

(4) Aime, S.; Botta, M.; Terreno, E. Gd(III)-Based Contrast Agents for MRI. *Adv. Inorg. Chem.* **2005**, *57*, 173–237.

(5) Bottrill, M.; Kwok, L.; Long, N. J. Lanthanides in Magnetic Resonance Imaging. *Chem. Soc. Rev.* **2006**, *35*, 557–571.

(6) Caravan, P. Strategies for Increasing the Sensitivity of Gadolinium Based MRI Contrast Agents. *Chem. Soc. Rev.* **2006**, *35*, 512–523.

(7) Hermann, P.; Kotek, J.; Kubiček, V.; Lukeš, I. Gadolinium(III) Complexes as MRI Contrast Agents: Ligand Design and Properties of the Complexes. *Dalton Trans.* **2008**, 3027–3047.

(8) Parker, D. Excitement in f Block: Structure, Dynamics and Function of Nine-Coordinate Chiral Lanthanide Complexes in Aqueous Media. *Chem. Soc. Rev.* **2004**, *33*, 156–165.

(9) Bünzli, J.-C. G.; Piguet, C. Taking Advantage of Luminescent Lanthanide Ions. *Chem. Soc. Rev.* **2005**, *34*, 1048–1077.

(10) Bünzli, J.-C. G. Benefiting from the Unique Properties of Lanthanide Ions. *Acc. Chem. Res.* **2006**, *39*, 53–61.

(11) de Bettencourt-Dias, A. Small Molecule Luminescent Lanthanide Ion Complexes−Photophysical Characterization and Recent Developments. *Curr. Org. Chem.* **2007**, *11*, 1460–1480.

(12) Gunnlaugsson, T.; Stomeo, F. Recent Advances in the Formation of Luminescent Lanthanide Architectures and Self-Assemblies from Structurally Defined Ligands. *Org. Biomol. Chem.* **2007**, *5*, 1999–2009.

(13) Bünzli, J.-C. G. Lanthanide Luminescent Bioprobes (LLBs). *Chem. Lett.* **2009**, *38*, 104–109.

(14) Montgomery, C. P.; Murray, B. S.; New, E. J.; Pal, R.; Parker, D. Cell-Penetrating Metal Complex Optical Probes: Targeted and Responsive Systems Based on Lanthanide Luminescence. *Acc. Chem. Res.* **2009**, *42*, 925–937.

(15) Caravan, P.; Astashkin, A. V.; Raitsimring, A. M. The Gadolinium(III)-Water Hydrogen Distance in MRI Contrast Agents. *Inorg. Chem.* **2003**, *42*, 3972–3974.

(16) Dewar, M. J. S.; Zoebisch, E. G.; Healy, E. F.; Stewart, J. J. P. Development and Use of Quantum Mechanical Molecular Models. 76. AM1: A New General Purpose Quantum Mechanical Molecular Model. *J. Am. Chem. Soc.* **1985**, *107*, 3902–3909.

(17) Dewar, M. J. S.; Zoebisch, E. G. Extension of AM1 to the halogens. *THEOCHEM* **1988**, *180*, 1–21.

(18) Dewar, M. J. S.; Yuan, Y.-C. AM1 parameters for sulfur. *Inorg. Chem.* **1990**, *29*, 3881–3890.

(19) For PM3, see: Stewart, J. J. P. Optimization of Parameters for Semiempirical Methods. I. Method. *J. Comput. Chem.* **1989**, *10*, 209–220.

(20) For La and Lu, see: Freire, R. O.; da Costa, N. B., Jr.; Rocha, G. B.; Simas, A. M. Sparkle/AM1 Structure Modeling of Lanthanum(III) and Lutetium(III) Complexes. *J. Phys. Chem. A* **2006**, *110*, 5897–5900.

(21) For Ce and Er, see: Freire, R. O.; do Monte, E. V.; Rocha, G. B.; Simas, A. M. AM1 Sparkle Modeling of Er(III) and Ce(III) Coordination Compounds. *J. Organomet. Chem.* **2006**, *691*, 2584–2588.

(22) For Pr, see: Freire, R. O.; da Costa, N. B., Jr.; Rocha, G. B.; Simas, A. M. Modeling Lanthanide Coordination Compounds: Sparkle/AM1 Parameters for Praseodymium(III). *J. Organomet. Chem.* **2005**, *690*, 4099–4102.

(23) For Nd, see: Bastos, C. C.; Freire, R. O.; Rocha, G. B.; Simas, A. M. Sparkle Model for AM1 Calculation of Neodymium(III) Coordination Compounds. *J. Photochem. Photobiol. A* **2006**, *177*, 225–237.

(24) Sm Freire, R. O.; da Costa, N. B., Jr.; Rocha, G. B.; Simas, A. M. Sparkle/AM1 Parameters for the Modeling of Samarium(III) and Promethium(III) Complexes. *J. Chem. Theory Comput.* **2006**, *2*, 64–74.

(25) For Eu, Gd, and Tb, see: Freire, R. O.; Rocha, G. B.; Simas, A. M. Sparkle Model for the Calculation of Lanthanide Complexes: AM1 Parameters for Eu(III), Gd(III), and Tb(III). *Inorg. Chem.* **2005**, *44*, 3299–3310.

(26) For Dy, see: da Costa, N. B., Jr.; Freire, R. O.; Rocha, G. B.; Simas, A. M. Sparkle model for the AM1 calculation of dysprosium(III) complexes. *Inorg. Chem. Commun.* **2005**, *8*, 831–835.

(27) For Ho, see: da Costa, N. B., Jr.; Freire, R. O.; Rocha, G. B.; Simas, A. M. Sparkle/AM1 modeling of holmium(III) complexes. *Polyhedron* **2005**, *24*, 3046–3051.

(28) For Tm, see: Freire, R. O.; Rocha, G. B.; Simas, A. M. Modeling rare earth complexes: Sparkle/AM1 parameters for thulium(III). *Chem. Phys. Lett.* **2005**, *411*, 61–65.

(29) For Yb, see: Freire, R. O.; Rocha, G. B.; Simas, A. M. Modeling lanthanide complexes: Sparkle/AM1 parameters for ytterbium (III). *J. Comput. Chem.* **2005**, *26*, 1524–1528.

(30) McNamara, J. P.; Berrigan, S. D.; Hillier, I. H. Semiempirical Molecular Orbital Scheme To Study Lanthanide(III) Complexes: PM3 Parameters for Europium, Gadolinium, and Ytterbium. *J. Chem. Theory Comput.* **2007**, *3*, 1014–1027.

(31) For PM6, see: Stewart, J. J. P. Optimization of Parameters for Semiempirical Methods V: Modification of NDDO Approximations and Application to 70 Elements. *J. Mol. Model.* **2007**, *13*, 1173–1213.

(32) For PM6/SPARKLE, see: Freire, R. O.; Simas, A. M. to be submitted.

(33) Freire, R. O.; Rocha, G. B.; Simas, A. M. Lanthanide complex coordination polyhedron geometry prediction accuracies of ab initio effective core potential calculations. *J. Mol. Model.* **2006**, *12*, 373–389.

(34) Under "real" structures, we understand the corresponding crystal structures for the purpose of this investigation. The estimated standard deviations as determined by single crystal X-ray diffraction in bond lengths between lanthanoids and N- or O-donor ligands are usually well below 0.3%. Since the errors of the computational models are much bigger than the ones associated with the crystal structure values, we assume the latter to be negligible with the acknowledgment that this is an approximation.

(35) It has to be emphasized that the development of the semiempirical methods, as well as our structural system of reference, is based on crystal structures. Therefore, our results implicitly have only validity for the estimation of Ln−OH$_2$ bond lengths in crystal structures. Our findings do not and cannot in any way address, for example, structures in solution.

(36) Seitz, M.; Oliver, A. G.; Raymond, K. N. The Lanthanide Contraction Revisited. *J. Am. Chem. Soc.* **2007**, *129*, 11153–11160.

(37) Allen, F. H. *Acta Cryst. B* **2002**, *58*, 380–388; http://www.ccdc.cam. ac.uk (accessed Oct 14, 2009).

(38) Hovinen, J.; Guy, P. M. Bioconjugation with Stable Luminescent Lanthanide(III) Chelates Comprising Pyridine Subunits. *Bioconjugate Chem.* **2009**, *20*, 404–421, and references cited therein.

(39) Gunnlaugsson, T.; Leonard, J. P. Responsive Lanthanide Luminescent Cyclen Complexes: From Switching/Sensing to Supramolecular Architectures. *Chem. Commun.* **2005**, *311*, 4–3131, and references cited therein.

(40) In addition, a number of other conditions had to be fulfilled, for example, only trivalent lanthanoid centers and exclusively N- or O-donor ligands. For a full list, see Supporting Information.

(41) Whenever "AM1" is mentioned from here on, "AM1/SPARKLE" is implied (in analogy also for "PM3" and "PM6").

(42) *MOPAC 2009*, versions 8.366W and 9.015W; Stewart Computational Chemistry: Colorado Springs, CO, 2009; http://OpenMOPAC.net (accessed Oct 14, 2009).

(43) For details see the Supporting Information.

(44) Shapiro, S. S.; Wilk, M. B. An Analysis of Variance Test for Normality (Complete Samples). *Biometrika* **1965**, *52*, 591–611.

(45) Lilliefors, H. On the Kolmogorov−Smirnov test for normality with mean and variance unknown. *J. Am. Stat. Assoc.* **1967**, *62*, 399–402.

(46) Scott, D. On optimal and data-based histograms. *Biometrika* **1979**, *66*, 605–610.

(47) It should be emphasized that the errors listed are not solely the result of inadequacies of the computational models but also to a great extent a function of the statistical uncertainties due to the limited sample set sizes.

(48) The statistical analysis for individual lanthanoids in cyclen-derived **2** is not meaningful because of the small sample sizes.

(49) For comparison, typical errors for distances obtained from fitting of NMRD profiles for Gd-based MRI contrast agents are also about 5% (see refs 2 and 4).